creases, a pole location can be tracked on a root-locus in the complex s plane as shown in Fig. 4. When the first critical flow speed is reached, the root locus shows the pole on the s-plane imaginary axis.

The plate's parameters have the following values.[6] The aerodynamic center and the location of the elastic axis is $a = -0.4 \cdot b$. The mass center location is $x_\alpha = 0.2 \cdot b$. The plate's radius of gyration is $r_\alpha = 0.5 \cdot b$. The mass ratio is $\mu = 40$ and the semichord $b = 1$. The pure pitch and plunge resonances are $\omega_\alpha = 100$ rad/s and $\omega_h = 50$ rad/s, respectively.

Conclusion

The fractional calculus model overcomes much of the impractical nature of Theodorsen's function. The model is an accurate algebraic description of the transcendental Theodorsen's function and it leads to an excellent, closed form approximation of Wagner's function. Furthermore, the fractional calculus model has no poles on the principle sheet of the $\bar{s}$ plane that obviates the difficulties associated with the aerodynamic poles associated with traditional algebraic models of Theodorsen's function. These strengths enable the model to conveniently describe the effects of unsteady aerodynamic loads for general small perturbation airfoil motion in both the Laplace domain and the time domain.

References

[1]Edwards, J. W., Ashley, H., and Breakwell, J. V., "Unsteady Aerodynamic Modeling for Arbitrary Motion," *Proceedings of the 18th Structures, Structural Dynamics and Materials Conference*, March 21–23, 1977 and Dynamics Specialists Conf., March 24–25, 1977, San Diego, CA, *Technical Papers*, Vol. B, 1977, pp. 267–283 (AIAA Paper 77-451).

[2]Bagley, R. L., and Calico, R. A., "Fractional Order State Equations for the Control of Viscoelastically Damped Structures," *Journal of Guidance Control and Dynamics*, Vol. 14, No. 2, 1991, pp. 304–311.

[3]Oldham, K. B., and Spanier, J., *The Fractional Calculus*, Academic Press, Orlando, FL, 1974.

[4]Sears, W. R., *Collected Papers of W. R. Sears Through 1973*, Cornell Univ. Press, Ithaca, NY, 1973, p. 38.

[5]Mittag-Leffler, G., "Sur La Represèntation Analytique D'une Branch Uniforme D'une Function Monagine," *Acta Mathematica*, Vol. 29, 1905, p. 101.

[6]Edwards, J. W., "Unsteady Aerodynamic Modeling for Arbitrary Motions," *AIAA Journal*, Vol. 15, No. 4, 1977, pp. 593–595.

Downwash Measurements on a Pitching Canard-Wing Configuration

John E. Burkhalter*
Frank J. Seiler Research Laboratory,
U.S. Air Force Academy, Colorado 80840

Introduction

MUCH of the experimental work associated with unsteady flows has centered around the harmonic oscillations of a single lifting surface, usually rotated about the quarter chord, and the resulting changes in the flowfield surrounding the model.[1,2] Only a few investigations[3,4] have considered the translation and rotation of finite wings such as those encountered on real, full-size, fighter-type, supermaneuverable aircraft in deep stall. Probably the best summary of the state of the art using a theoretical approach is found in Refs. 5–7. In Ref. 5, a structured approach to the problems associated with a theoretical analysis of oscillating airfoils is provided in which the various terms in the force and moment equations are discussed along with a two-dimensional solution for simple harmonic motion. For the examples chosen in the analysis, prediction of phase angles, due to circulation lag, of about 15 deg for specific configurations seems to be typical. It was shown in Ref. 8 that the maximum lift coefficient experienced during sinusoidal oscillation changes drastically with alterations of the lifting surface rotation point. For the two-wing case, with the rotation point somewhere between the two wings, one would expect significant deviations from the quarter chord rotation point data. In a two-dimensional experiment by Walker,[9] a forward airfoil was pitched about its quarter chord axis at a constant rate. Flow visualization results indicated that the leading-edge vortex, separated from the forward airfoil section, could be made to pass either over or under an aft airfoil. In this tandem wing arrangement, such as those described in Ref. 9, the downwash loading from forward lifting surfaces can make significant contributions to the loading on a downstream wing or tail. Because downwash loads and moments are difficult to predict theoretically, especially for unsteady motions, a series of wind-tunnel tests were completed in a low-speed wind tunnel on a generic configuration as pictured in Fig. 1, in which attempts were made to measure downwash directly.[10]

The experimental wind-tunnel tests were conducted in a low-speed, open return wind tunnel. The test section was 3 × 3 ft (91.44 × 91.44 cm), and the nominal freestream velocity was 89 ft/s, producing a Reynolds number of about 2.05 × 10^5 based on the wing chord length of 6.0 in. All airfoil sections were NACA 0015, and the wings were mounted to individual load and moment balances at the quarter chord of each wing. The two wing assemblies, as shown schematically in Fig. 1, were mounted to an oscillating splitter plate connected to a shaft and bearing assembly in the floor of the wind-tunnel test section. The wings were mounted in the vertical direction for ease of construction and ready access to the drive assembly underneath the tunnel floor. The round splitter plate was beveled to a 30-deg angle to reduce boundary layer and hardware interference in the test data. Each wing was mounted to a shaft along the quarter chord which was rigidly attached to individual load and moment balances. This shaft, running through the quarter chord, also served as a means of setting each wing incidence angle. The bottom of each shaft was fixed to a rigid plate bolted directly to the face of each balance, and the plate was designed so that its upper surface was flush with the splitter plate surface. A small gap between the root or bottom end of the wing raised the wing to near the edge of the boundary layer on the oscillating plate.

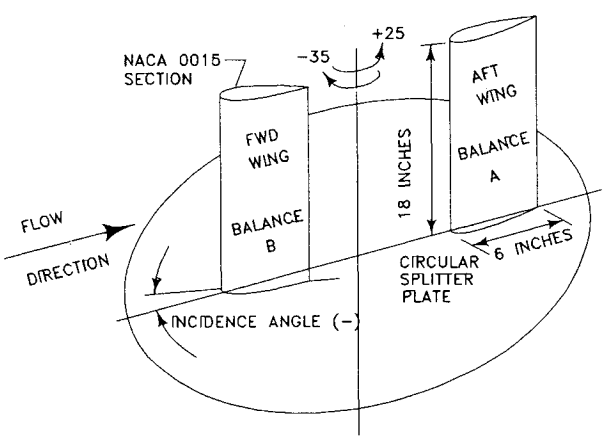

Fig. 1 Schematic of splitter plate model.

Received Sept. 9, 1991; revision received Dec. 14, 1992; accepted for publication Dec. 19, 1992.

*Visiting Professor; currently Associate Professor, Aerospace Engineering Department, Auburn University, AL. Senior Member AIAA.

The splitter plate was rigidly connected to a drive shaft supported by a large bearing assembly attached to the bottom of the tunnel. The drive shaft protruded through the bearing assembly and through the tunnel floor. The drive motor assembly consisted of a 1.0-hp variable speed dc motor connected to a gear reducer by means of a flexible coupling. The output of the gear reduction unit was connected to a flywheel-type connecting arm assembly which was rigidly attached to the output shaft protruding through the tunnel floor. The linkage system was so designed that one full revolution of the gear reduction output arm produced a 60-deg swing in the splitter plate. Because of the design dimensions, the plate rotation was limited to about +25 and −35 deg.

Sensors for the experiment consisted of two five-component load balances, a bridge circuit assembly for the angle measurements, the wind-tunnel speed transducer, and an optical encoder. Only three components on each balance were used consisting of 1) normal force, 2) pitching moment, and 3) rolling moment (root chord bending moment). A bridge circuit was used to measure the angular position of the plate and the optical encoder was used to "start" the measuring cycle at a precise location of the splitter plate.

A high-speed computer digitized each channel of data at a rate of 1.0 MHz and stored the data in memory for later processing. Clock pulses were generated internally to the computer to start each "burst" of data at predetermined time steps during each cycle. At each clock pulse, each channel was sampled four times at the 1.0-MHz rate. Each data cycle was repeated four times to produce aggregate data which was averaged in order to eliminate "some" of the scatter in the data and to eliminate some of the electronic noise. The data were also electronically filtered using a low pass filter to further eliminate electronic noise. Clock pulse frequencies were adjusted to correspond to approximately 30 data sets (angular positions of the splitter plate), depending on the preset rotation rate of the drive motor. It was assumed that the clock pulses occurred at the same angular positions of the splitter plate during each of the four cycles so that data from each cycle could be averaged. After all data from each cycle was stored in memory, postprocessing of the data produced final coefficients, numerically differentiated angular velocities, and corrected angular positions. For all cases, data were taken only for the upswing of the splitter plate. Because of the particular setup in the wind tunnel, it was not possible to take data on both the upswing and downswing cycle of the splitter plate.

The mechanism was rotated at differing rates with tunnel air off, and the resulting data was stored in a three-dimensional array which served as the "zero data" file. In order to extract a single channel zero reading, a double linear interpolation was required in the three-dimensional array, depending on measured angular position and measured angular rotation rate. In this manner, the inertial and electronic offset loads and moments were subtracted from the wind on data resulting in a measurement of the aerodynamic loads alone. For each new configuration in which the inertial loads would change, a new zero data file was generated. The data as presented in the following figures were obtained from individual balances attached to each wing. In some cases these data were extracted from two runs in order to obtain the actual downwash loading.

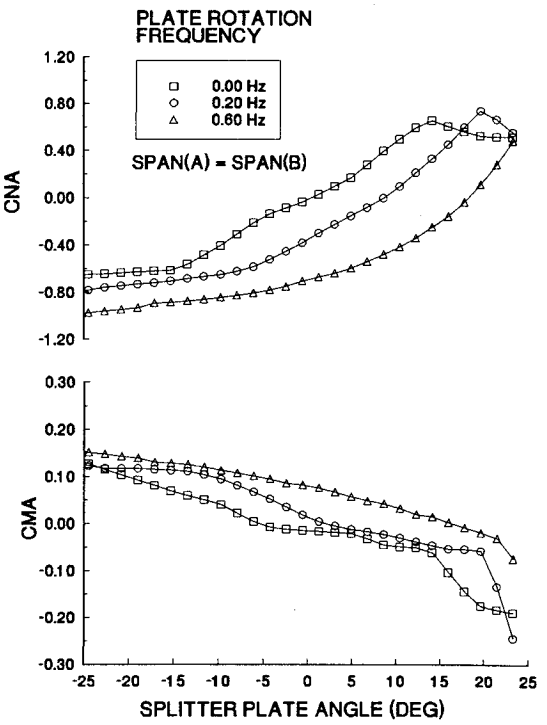

Fig. 2 Aft wing normal force and pitching moment coefficients vs splitter plate angle, equal semispans.

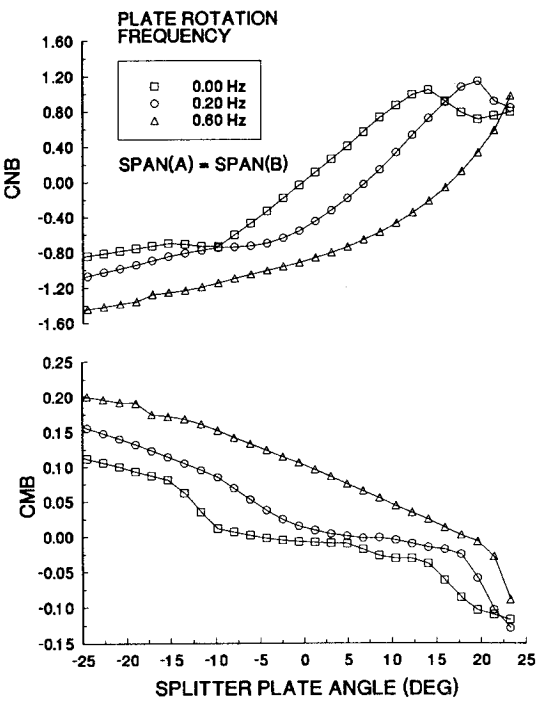

Fig. 3 Forward wing normal force and pitching moment coefficients vs splitter plate angle, equal semispans.

Results

As pointed out in Ref. 5, unsteady oscillations cause a delay or lag in the loading on two-dimensional airfoils. This is also true of finite wings and is even more pronounced for rotation about a point not on the airfoil section. Figures 2 and 3 are plots of experimental normal force and pitching moment coefficient data for a two-wing configuration of equal span. The normal force coefficient was defined in the standard manner with the reference area being the wing planform area of the largest wing tested (18-in. semispan and a 6-in. chord). The distance from the rotation point in the middle of the splitter plate to the leading edge of the forward and aft wings was 8 in. (1.33 chord lengths). Data were taken during the oscillation as the plate traverses a negative to positive rotation angle. Because of the electronic setup and computer averaging of the data, it was not possible to take data in the positive to negative direction rotation of the splitter plate. The steady-state data, 0.0-Hz case, indicated that the wing stalled at about 14 deg for both the forward and aft wings as shown in Figs. 2 and 3. As the plate rotation rate was increased to 0.2 and

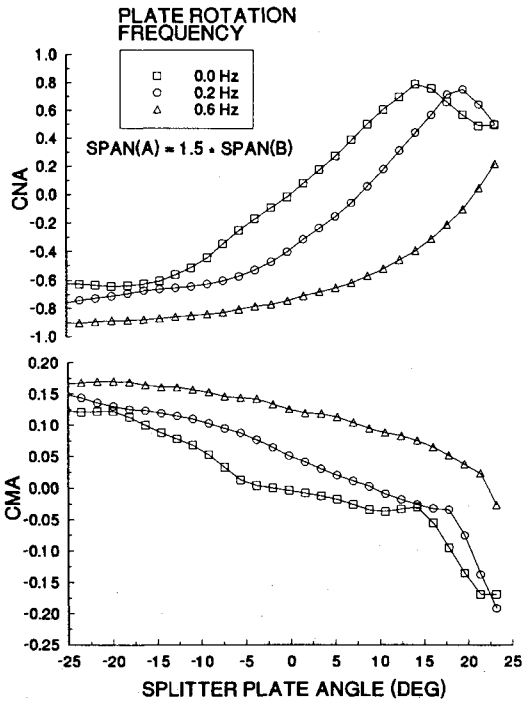

Fig. 4 Aft wing normal force and pitching moment coefficients vs splitter plate angle, unequal semispans.

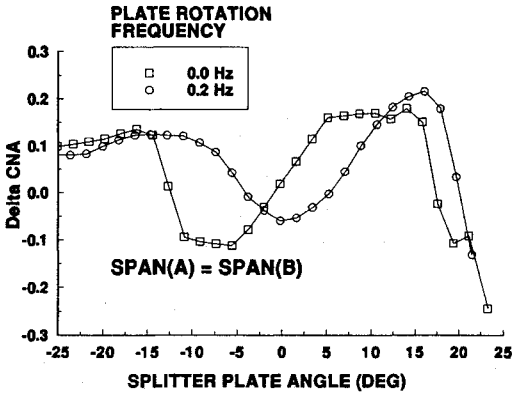

Fig. 5 Aft wing downwash coefficients vs splitter plate angle, steady and unsteady states, equal semispans.

0.6 Hz, the stall angle for both wings shifted to higher and higher angles of attack. It is clear, from Figs. 2 and 3, that this lag in the loading was a nonlinear function, dependent on the airfoil rotation rate, the angle of attack history, and the relative rotation axis location. These results and those of Refs. 3, 11, and 12 clearly point out that the pivot radius is a critical factor in unsteady measurements and must be included in comparing data for oscillating airfoils and wings.

Changing the semispan of the forward wing did not appear to alter the results as shown in Fig. 4. Therefore, it appears that this lag in the loading was primarily a two-dimensional phenomenon dependent on the shed vorticity in the chordwise direction, and essentially independent of the vortex trailing legs from the forward wing. It may also be concluded that the loading lag on an aft wing is only weakly influenced by the presence of an additional lifting surface. This is not to say, however, that the loading lag and downwash are not in some way coupled, as will be shown later. It is clear from these results that the stall angle increases significantly with increases in rotation rate. However, the delineation between the "lift" stall and the "moment" stall, hypothesized in Ref. 13, was not clearly depicted in the data. There is some hint of a difference in comparing Figs. 2 and 3.

Though somewhat complicated, the downwash can be measured directly in the steady or unsteady case. First, coefficients for the wing of interest, say the aft wing, must be obtained with and without the "inducing" front wing present. Of course, this approach does not yield localized flowfield results, but does provide global changes in the aerodynamic coefficients. For the present experiments, only the normal force, pitching moment, and root chord bending moment (rolling moment) were measured. Figure 5 is a typical output for the case of two 18-in. wings as pictured schematically in Fig. 1. A positive downwash is defined to be downward directed, resulting in a negative value for Delta CNA, where Delta CNA is defined to be the change in normal force coefficient on the aft wing due to downwash from the forward wing. When the whole system is oscillated at some positive splitter plate rotation frequency, the maximum value of the magnitude of the downwash changes very little due to a nonzero reduced frequency. This can perhaps be explained by noting that the downwash is probably masked by changes in loading due to "circulation lag"; the term circulation lag refers to that part of the wing loading due to circulation. Secondly, even though the magnitude of the downwash changes very little, the downwash curve is shifted in angle of attack to the right. That is, maximum upwash does not occur at a negative stall angle, but for this particular case occurs at near zero angle of attack. The shift in the downwash curve is essentially the same as the shift in alpha due to the lag in circulation on the aft wing section. That is, the shift in the downwash curve is due to circulation lag of the aft wing coupled with the loading on the forward wing.

From the present test results the following conclusions are made:

1) The loading due to circulation lag associated with oscillating wings is an important fundamental property of the flowfield. It is essentially independent of external induced downwash flowfields, but is dependent on the location of the pivot point for the wing or airfoil section, the relative rotation rate, and the angle-of-attack history of the lifting surface.

2) Downwash from a forward wing on an aft lifting surface can enhance or degrade the potential of an aft wing to produce lift.

3) In an oscillating two-wing configuration, both the forward and aft wing lift are affected by the circulation lag. The downwash induced on the aft wing is not synchronized with the circulation lag of the downwash producing front wing, but rather with the circulation lag of the aft wing. Consequently, a forward wing producing positive lift can produce upwash on the aft wing increasing its potential to produce lift.

References

[1]Ashworth, J., Mouch, T., and Luttges, M., "Application of Forced Unsteady Aerodynamics to a Forward Swept Wing X-29 Model," AIAA Paper 88-0563, Jan. 1988.

[2]Ashworth, J., Crisler, W., and Luttges, M., "Vortex Flows Created by Sinusoidal Oscillation of Three-Dimensional Wings," AIAA Paper 89-2227, July–Aug. 1989.

[3]Ohmi, K., Coutanceau, M., Daube, O., and Ta Phuloc Loc, "Further Experiments on Vortex Formation Around an Oscillating and Translating Airfoil at Large Incidence," *Journal of Fluid Mechanics*, Vol. 225, April 1991, pp. 607–630.

[4]Ohmi, K., Coutanceau, M., Ta Phuloc Loc, and Dulieu, A., "Vortex Formation Around an Oscillating and Translating Airfoil at Large Incidence," *Journal of Fluid Mechanics*, Vol. 211, Feb. 1990, pp. 37–60.

[5]Ericsson, L. E., and Reding, J. P., "Fluid Mechanics of Dynamic Stall, Part I. Unsteady Flow Concepts," *Journal of Fluids and Structures*, Vol. 2, 1988, pp. 1–33.

[6]Ericsson, L. E., and Reding, J. P., "Fluid Mechanics of Dynamic Stall, Part II. Prediction of Full-Scale Characteristics," *Journal of Fluids and Structures*, Vol. 2, 1988, pp. 113–143.

[7]Katz, J., and Maskew, B., "Unsteady Low Speed Aerodynamic Model for Complete Aircraft Configurations," *Journal of Aircraft*, Vol. 25, No. 4, 1988, pp. 302–310.

[8]Visbal, M. R., and Shang, J. S., "Investigation of the Flow Struc-

ture Around a Rapidly Pitching Airfoil," *AIAA Journal*, Vol. 27, No. 8, 1989, pp. 1044–1051.

[9]Walker, J., "Dynamic Stall Wake Interaction with a Trailing Airfoil," AIAA Paper 87-0239, Jan. 1987.

[10]Burkhalter, J. E., "Downwash Measurements on a Pitching Canard-Wing Configuration," Final Rept., Frank J. Seiler Research Lab., FJSRL TR-91-0001, USAFA, CO, Sept. 1991.

[11]Stephen, E., Walker, J., Roh, J., Eldred, T., and Beals, M., "Extended Pitch Axis Effects on the Flow About Pitching Airfoils," AIAA Paper 89-0025, Jan. 1989.

[12]Helin, H. E., and Walker, J. M., "Interrelated Effects of Pitch Rate and Pivot on Airfoil Dynamic Stall," AIAA Paper 85-0130, Jan. 1985.

[13]McAlister, K. W., Carr, L. W., and McCroskey, W. J., "Dynamic Stall Experiments on the NACA 0012 Airfoil," Ames Research Center, NASA TP 1100, Moffett Field, CA, 1978.